ELSEVIER

Thin Solid Films 333 (1998) 245–250

thin solid films

Defect distribution and evolution in He^+ implanted Si studied by variable-energy positron beam

Miao Zhang[a,*], Chenglu Lin[a], Huiming Weng[b], R. Scholz[c], U. Gösele[c]

[a]*State Key Laboratory of Functional Materials for Informatics, Shanghai Institute of Metallurgy, Chinese Academy of Sciences, Shanghai 200050, People's Republic of China*

[b]*Department of Modern Physics, University of Science and Technology of Chinxxa, Hefei 230026, People's Republic of China*

[c]*Max-Plank-Institute of Microstructure Physics, Weinberg 2, D-06120, Hale, Germany*

Received 22 September 1997; accepted 9 April 1998

Abstract

The distribution and annealing behavior of the vacancy-type defects and displaced Si atoms in crystal Si caused by 7×10^{16} cm^{-2}, 140 keV He^+ implantation have been studied by variable-energy positron annihilation technology, cross-sectional transmission electron microscopy and Rutherford backscattering and channel spectroscopy. It was found that in the as-implanted sample, a region 400 nm wide around the projected range was heavily damaged by the implantation and dense microbubbles with diameters of 1.5–6 nm were formed in this region, while the near surface region was slightly damaged and small vacancy clusters less than 1 nm in diameter and some microbubbles scattered in this region. The defects in the heavily damaged region were stable at temperature below 400°C and began to recrystallize from the crystalline Si in the near surface layer by solid phase epitaxy at temperatures higher than 600°C. High temperature (1100°C) was needed to anneal out most of the defects in this heavily damaged layer. The small vacancy clusters in the near surface region become removable at 300°C and could be removed at 700°C by dissociation and diffusing both to the surface and to the heavily damaged region. The diameter of the microbubbles in the original heavily damaged region increased with the increasing of annealing temperature and their density decreased with the increasing of annealing temperature at temperatures above 700°C. The annealing behavior of the vacancy clusters induced by He^+ implantation is discussed by thermodynamical process.

Keywords: Positron spectroscopy; Rutherford backscattering spectroscopy; Transmission electron microscopy; Vacancies

1. Introduction

High dose of He^+ implanted into silicon will produce a bubble layer near the ion projected range [1]. During the post annealing treatment, He in these bubbles will release out, leaving empty voids in the bulk of the samples. These voids have been demonstrated to be strong gettering sites for transitional metal impurities [2–5]. A recent study of Raineri and Campisano shows that these voids even can act as traps for interstitial during high temperature annealing [6]. The gettering effect of voids to transitional metals and to interstitial has potential applying for very large scale integrated (VLSI) devices and thus has stimulated further studies in this field. The morphology of voids has been studied by cross-sectional transmission electron microscopy (XTEM) [2–5]. However, small vacancy clusters less than 1 nm in diameter cannot be observed by XTEM. Among the different techniques used to study the structural disorder caused by ion implantation, variable-energy positron annihilation spectroscopy (VEPAS) and Rutherford backscattering spectroscopy in the channeling geometry (RBS/C) are very powerful techniques. The former is very sensitive to vacancy defects, and the latter provides information on atom displacement.

VEPAS has been successfully used recently as a sensitive method for depth profiles of near-surface defect induced by ion implantation [7–10]. This technique is based on the fact that positrons, when implanted at a given energy, thermalize and diffuse inside the medium, and finally annihilate with electrons, producing two γ photons with energy of 511 keV. Doppler-broadened profile of these γ photons can provide information about the existence of vacancy-type defects. A slow positron beam consists of variable energetic positrons of which the energy can be varied by adjusting the accelerating voltage. Variable-energy positrons could be implanted into the films at different depths. By detecting the annihilation photons, one can obtain the depth distribution of vacancy type defects. Comparing with other techni-

* Corresponding author. Tel.: +86 21 62511070; fax: +86 21 62513510.

0040-6090/98/$ - see front matter
PII S0040-6090(98)00808-6

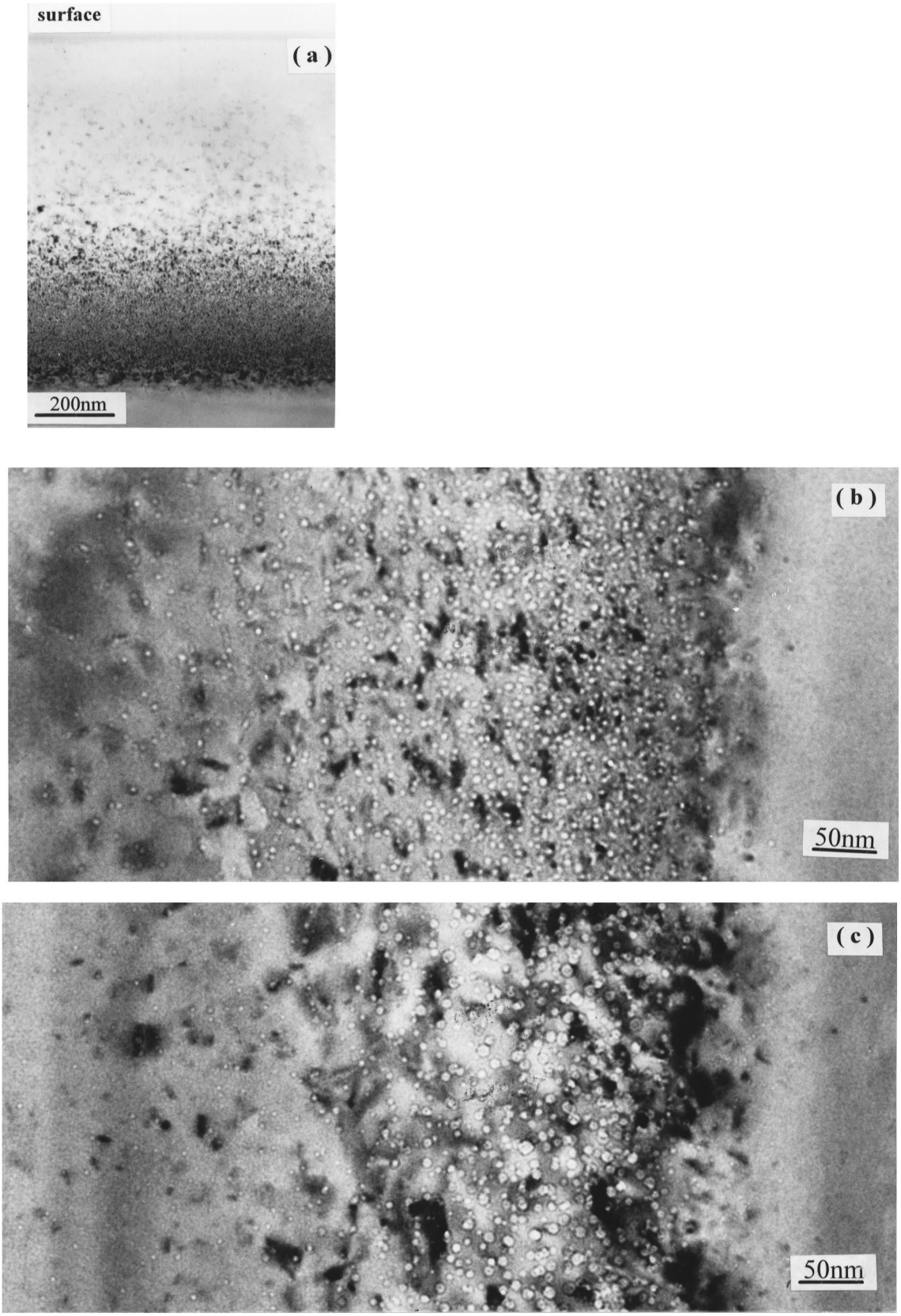

Fig. 1. XTEM image of the 7×10^{16} cm^{-2} He^{+} implanted sample. (a) As-implanted, the heavily damaged layer situates at 550–940 nm from the surface, (b) as-implanted image at higher magnification, microbubbles can be clearly observed and (c) annealed at 700°C for 30 min, larger voids have formed.

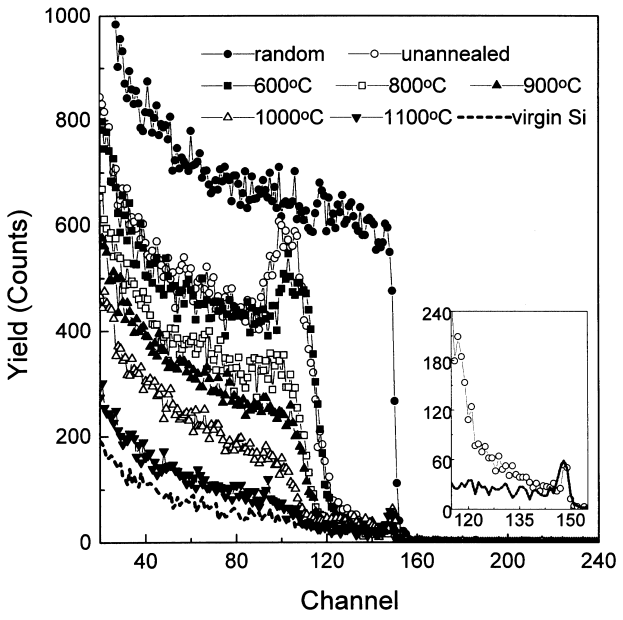

Fig. 2. The RBS/C spectra of the samples implanted with 7×10^{16}cm^{-2} He^+ at 140 keV and annealed at different temperatures. The channeling spectrum of a virgin Si is also shown for comparison. The insert gives the magnified RBS/C spectra of the He^+ as-implanted sample and the virgin Si.

ques, VEPAS is an unique non-destructive method with an high defect sensitivity at low damage level. In this paper, XTEM, RBS/C and VEPAS have been combined to investigate the He-implantation-induced defects distribution in He-implanted c-Si as well as their evolution with annealing temperature.

2. Experimental

p-Type (100) CZ Si with a resistivity of 20–35 Ω·cm was implanted with He^+ ions at room temperature with an energy of 140 keV and dose equal to 7×10^{16} cm^{-2}. During the implantation, a deliberate beam misalignment from the wafer normal equal to 7° was used. The twist angle was 0°. Then the sample was annealed in the temperature range of 100–1100°C for 30 min in the ambient of N_2 gas.

The samples before and after annealing were investigated by XTEM, VEPAS and 2-MeV He^+ RBS/C. The scattering angle during the RBS/C was 160°. The cross-section specimens were studied by 200-kV CM-20 and 400-kV JEM-400EX microscopes. VEPAS measurements were carried out in an ultrahigh vacuum chamber (4×10^{-7} Torr) using a positron variable-energy beam system from a ^{22}Na source. In each measurement 10^5 counts were accumulated. The positron energy could be varied from 0.5 to 16 keV by adjusting the voltage applied to the target. An energy-sensitive γ-ray germanium detector was used to determine the Doppler-broadened annihilation spectra caused by the momentum of the annihilating positron-electron pairs. The shape of the spectra were characterized by a line-shape parameter S, which is defined as the area of a fixed central region of the 511 keV line divided by the total area of the peak. We took an energy shift $a = 1$ keV at both sides of the peak energy of 511 keV.

3. Results and discussion

Fig. 1 exhibits the XTEM images of the 7×10^{16} cm^{-2} He^+ implanted samples before and after annealing. Fig. 1a shows the microstructure of the as-implanted sample, in which a severely damaged region has been generated at a depth between 550 and 940 nm from the surface. The projected range of 140 keV He^+ implants calculated by TRIM 94 program is 850 nm. The near surface region is slightly damaged. The heavily damaged region mainly consists of microbubbles of high density. These bubbles can be seen more clearly at higher magnification of thinner specimen in the out-off-focus condition, as shown in Fig. 1b. The diameters of the bubbles are in the range of about 1.5 to 6 nm. Towards the surface a decreasing density of small microbubbles was observed and such microbubbles can be occasionally observed at a depth of 250 nm from the surface. After annealing at 700°C for 30 min an increase of the bubble (or void) diameters (now about 4–11 nm) and a decrease of their density were observed in the original severely damaged region as shown in Fig. 1c which is at the same magnification as that in Fig. 1b. The voids present in the surface region of the 700°C annealed sample shrank in size (2 nm in diameter), while the void population decreased. Since the implanted He effuses out from the bubbles at temperature higher than 700°C [1,4,11], the 'bubbles' observed in Fig. 1c are empty voids. After the 700°C annealing the large bubbles in the heavily damaged region are confined in a narrower band 300 nm wide.

The RBS/C spectra of the He^+ implanted samples before and after thermal treatment are given in Fig. 2. The channeling spectrum of a virgin Si was also shown for comparison. The channeling spectrum of the as-implanted sample in Fig. 2 clearly indicates the presence of a severely damaged region below a surface region still crystalline. Therefore, most of the microbubbles observed in Fig. 1a,b are situated in a heavily damaged region. When the implanted samples were annealed in the temperature interval from 100 to 400°C, no obvious change has been detected in the buried damaged region by RBS/C, indicating that such a damage is stable in this temperature range. Increasing the annealing temperature to 600°C, the dechanneling yield from the damaged layer decreases, suggesting that the damaged layer begins to recover. Annealed at higher temperature (800–1000°C), the dechanneling yield from the damaged layer continues to decrease, accompanied by the inwards movement of the front edge of the damaged layer. This phenomenon strongly suggests that the damage recovers at higher temperatures, in the meanwhile it regrows epitaxially from the undamaged surface layer. After the

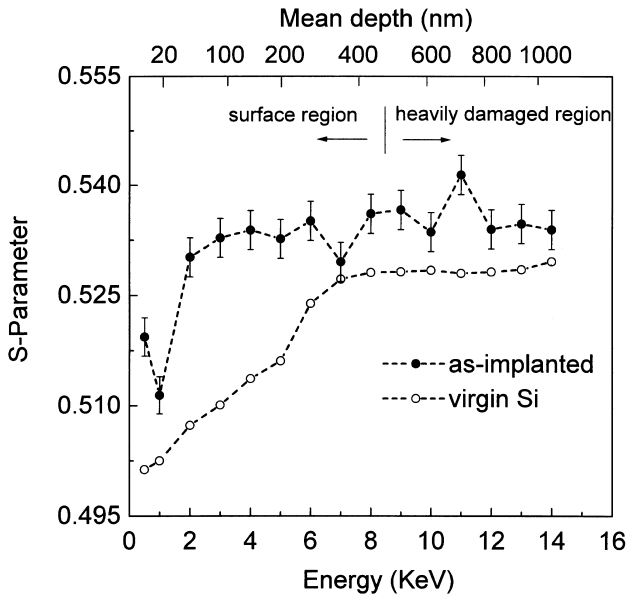

Fig. 3. The *S* parameter as a function of the positron energy for the 7×10^{16} cm^{-2} He^+as-implanted Si and the virgin Si, which is displayed for comparison. The upper horizontal axis gives the mean implantation depth of the positrons.

1100°C annealing, most of the initial He^+ implantation induced damage has been annealed out, leaving the cavities embedded in good crystalline Si. The insert in Fig. 2 gives the magnified RBS/C spectra for the as-implanted sample and the virgin Si. The dechanneling yield in the near surface of the as-implanted sample exhibits a tendency to increase, suggesting that the near surface has been slightly damaged by the high-dose of He^+ implantation. This result is in good agreement with the XTEM observations.

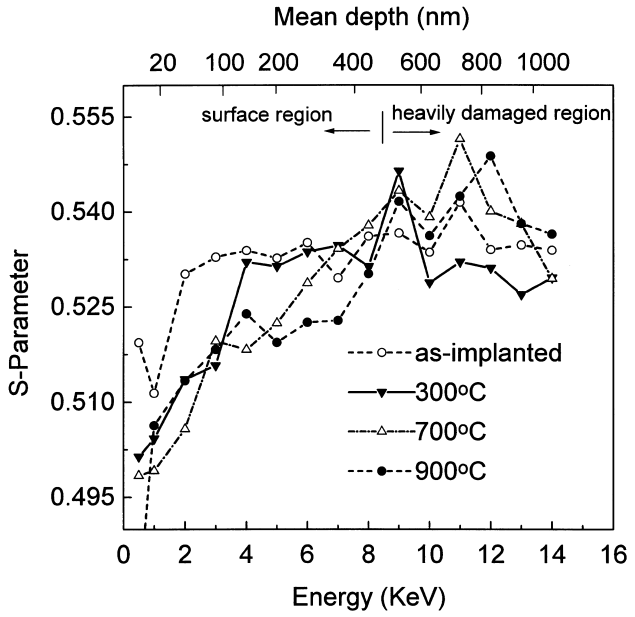

Fig. 4. The *S–E* results of the sample implanted with 7×10^{16} cm^{-2} $He^+$and annealed at various temperatures. The upper horizontal axis gives the mean implantation depth of the positrons.

Fig. 3 shows the positron annihilation line shape parameter *S* as a function of the positron energy (*E*) for the virgin Si and the He^+ ions as-implanted sample. In Fig. 3 the error bars for the He^+ as-implanted sample are given. The unimplanted sample exhibits the usual behavior of a defect free crystalline silicon. The *S* parameter values of the virgin Si increase slowly in the surface region and reach a bulk value of 0.528 at a depth of 350–430 nm and then keep the constant value S_{bulk}, while the *S* parameter values of the He^+ as-implanted specimen increase rapidly to 0.53 at a depth of 50 nm from the surface and reach the highest value of 0.541 at $D = 720$ nm.

The differences in these two sets of data are ascribed to positrons annihilating in different traps. Generally, the positrons implanted in the sample have three paths to be annihilated: (i) annihilated in the vacancy-free bulk, the S_{bulk} is a characteristic parameter for the material; (ii) trapped by vacancy-type defects, giving a higher S_{vac} value than S_{bulk}, and (iii) diffused to the sample surface, giving a lower S_{surf} than S_{bulk} ($S_{surf} < S_{bulk} < S_{vac}$) [12].

$$S(E) = f_{surf}S_{surf} + f_{vac}S_{vac} + f_{bulk}S_{bulk} \quad (1)$$

and $f_{surf} + f_{vac} + f_{bulk} = 1$, where f_{surf}, f_{vac} and f_{bulk} are the fraction of positrons annihilating at the surface, in the vacancy-type defects and in the bulk, respectively. For the unimplanted sample, the measured *S* parameter increases slowly with positron energy until the bulk value is reached. This is a consequence of the fact that with increasing energy, the positrons are implanted deeper and deeper inside the sample, fewer and fewer positrons will diffuse to and annihilate at the surface. Almost all of the positrons implanted with energy higher than 8 keV annihilate in the bulk freely, giving a constant value of S_{bulk}. In the ion implanted samples, vacancies have been generated. Because the *S* value of positrons annihilate at vacancy-type defects is larger than S_{bulk}, the presence of vacancies will result in higher *S* value than that in the virgin sample. Therefore the abrupt increase of the *S* value in the He^+ as-implanted at 50 nm should be attributed to the presence of a high density of vacancy-type defects. Since no microbubbles can be observed at this depth by XTEM, we infer that the vacancy-type defects in this region are small vacancy clusters with diameters less than 1 nm. This result demonstrates that VEPAS is very sensitive to small vacancy-type defects which cannot be observed by XTEM.

The *S–E* curves of the samples annealed in temperature from 300 to 900°C are reported in Fig. 4. The result of the as-implanted specimen is also shown for comparison. The *S–E* curves can be divided into two regions according to their different annealing behavior: the near surface region ($0 < D < 550$ nm) and the deep damaged region (550 nm $< D <$ 1000 nm). In the 300°C annealed sample, an abrupt decrease of the *S* parameter at 50~150 nm was observed. This phenomenon indicates that some of the

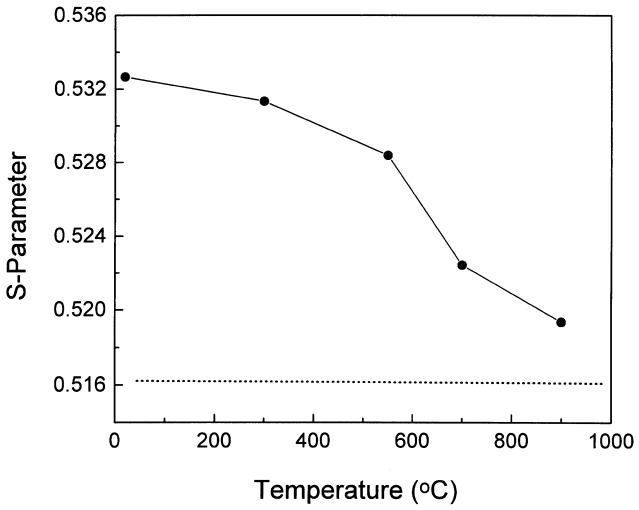

Fig. 5. Variation of S parameters at $E = 5$ keV (200 nm) for the sample implanted with 7×10^{16} cm^{-2} He^{+}and annealed at various temperatures. The S parameter of the virgin Si at the same depth was given in dash for reference.

vacancy-type defects in this region have been removed. Among the vacancy-type defects induced by ions implantation in Si, divacancies are known to be the dominant defects and become mobile at 200–300°C [13]. Therefore, we propose that the species of the vacancy-type defects in this region are divacancy. Increasing the annealing temperature, the S parameters at deeper location began to decrease. Annealed at 700°C, the S parameter at $D = 350$ nm was lower than that of the as-implanted sample, suggesting that some of the vacancies at this depth began to be annealed out. After the 900°C annealing, all of the S parameters at $D < 550$ nm have been greatly decreased and the high S values exist in a narrower region. The S parameters at $D =$ 200 nm as a function of annealing temperature were given in Fig. 5. The S parameter of the virgin Si at the same depth was given for reference. It can be seen that the S parameter at $D = 200$ nm decreases with the increasing of the annealing temperature.

Based on the annealing behavior of defects in the surface region, we argue that different kind of vacancy-type defects have generated along the path of the implants. The deeper, the vacancy cluster (V_n) is bigger, and higher temperature is needed to remove these clusters. The main vacancy defects in $D = 50$–150 nm are divacancy (V_2), while the vacancy-type defects around the projected range are microbubbles with diameters higher than 1.5 nm. Upon annealing the small vacancy clusters probably dissolve and the associated vacancies diffuse to the bubbles, contributing to the growth of the microbubbles (voids).

The S–E curves in the heavily damaged region appear rather complex. Density microbubbles have been formed in the heavily damaged layer of the He^{+} as-implanted sample (Fig. 1). Therefore, it is expected that high S parameters should be obtained in this bubble layer. Surprisingly, we found that the parameter in this region only exhibited a small peak at $D = 720$ nm. The reason for this phenomenon is not clear but may be related to the presence of He in the bubbles. Similar phenomenon has been observed by Smith et al. [14] and Brusa et al. [15] in the H^{+}-implanted silicon. They found that no positron trapping was detected in the damaged region containing dislocation loops, platelets cavities and small bubbles. However, we found that at temperatures higher than 700°C, the S parameters in the cavity layer have obviously increased. This may be related to the out-diffuse of He from the bubbles and to the coalescence of the voids.

Combing the results of XTEM, RBS/C and VEPAS, we propose the following mechanism to interpret the annealing behavior of the high-dose He^{+} implantation induced defects in Si. In the as-implanted samples, most of the defects (vacancies and interstitial) are concentrated near the projected range, the density of defects in the near surface region is low. The study of Raineri et al. has demonstrated that bubbles can only form in the region where the local concentration of He implants exceeds 3.5×10^{20} cm^{-3} [2]. Therefore, in the He^{+} as-implanted sample bubbles are mainly formed near the projected range, and small vacancy clusters which cannot be observed by XTEM are the dominant defects in the near surface region. The annealing behavior of the vacancy-type defects can be explained by thermodynamical consideration. During annealing, both the dissociation of the small vacancy clusters and the coalescence of the bubbles take place. In order to minimize the total surface energy of the vacancy clusters, small clusters dissolve and large clusters grow from the dissolved vacancies. At a given temperature, there exists a critical radius, r_c, for the vacancy cluster. Below this r_c, the vacancy clusters will dissociate, above this r_c the cluster is stable.

$$r_c = -\frac{2\sigma}{\Delta H_v}\frac{T_E}{T_E - T} \tag{2}$$

where T is the temperature, T_E is the temperature of equilibrium between the two phase of vacancies (vacancy in 'precipitates' (voids) and in silicon solution), ΔH_v is the volume enthalpy of formation of the vacancy clusters, and σ is the surface energy of the clusters. r_c increases with temperature. Small clusters dissociate at low temperature, and the dissolving of larger clusters needs higher annealing temperature. This mechanism can interpret the fact that divacancies dissolve at relatively low temperature of 200–300°C and that the migration and coalescence of voids observed by XTEM only occur at temperature higher than 700°C [1].

4. Conclusion

In this study, the defects distribution and annealing behavior in the He^{+}-implanted crystal Si have been studied by XTEM, RBS/C and VEPAS and we have reached the following conclusions. (i) In the as-implanted Si, a heavily

damaged region in which microbubbles embedded has formed around the projected range, and small vacancy clusters have generated in the slightly damaged near surface. (ii) Annealed at a temperature interval of 100–900°C, the small vacancy clusters with diameters less than 1 nm in the surface region dissolve and diffuse to the originally heavily damaged region and the voids dispersed in the surface region were observed shrinking in size, while the bubbles (voids) of high density around the projected range coarsen with the increasing of annealing temperature, and (iii) the heavily damaged region is stable at temperature below 400°C and recrystallizes by solid phase epitaxy from the surface crystalline silicon at temperatures higher than 600°C. This severely damaged region recovered at 1100°C.

References

[1] C.C. Grriffioen, J.H. Evens, P.C. De Jong, A. Van Veen, Nucl. Instrum. Methods B 27 (1987) 417.
[2] V. Raineri, P.G. Fallica, G. Percolla, et al., J. Appl. Phys. 78 (6) (1995) 3727.
[3] V. Raineri, A. Battaglia, E. Rimini, Nucl. Instrum. Methods B 96 (1995) 249.
[4] D.M. Follstaedt, S.M. Myers, G.A. Petersen, J.W. Medernach, J. Electron. Mater. 25 (1) (1996) 151.
[5] S.A. McHugo, E.R. Weber, S.M. Myers, G.A. Petersen, Appl. Phys. Lett. 69 (20) (1996) 3060.
[6] V. Raineri, S.U. Campisano, Appl. Phys. Lett. 69 (12) (1996) 1783.
[7] M. Fujinami, Phys. Rev. B 53 (19) (1996) 13047.
[8] M. Fujinami, A. Tsuge, K. Tanaka, J. Appl. Phys. 79 (12) (1996) 9017.
[9] G. Ghislotti, B. Nielsen, P. Asoka-kumar, et al., Appl. Phys. Lett. 70 (4) (1997) 496.
[10] K.C. Hall, R.D. Goldberg, T.D. Lowes, et al., Can. J. Phys. 74 (1996) S248.
[11] P.F. Fichtner, J.R. Kaschny, R.A. Yankov, et al., Appl. Phys. Lett. 70 (1997) 732.
[12] J. Keinonen, M. Hautala, E. Rauhala, V. Karttunen, A. Kuronen, J. Raisanen, Phys. Rev. B 37 (1988) 8269.
[13] A. Uedono, S. Tanigawa, M. Ogasawara, Jpn. J. Appl. Phys. 29 (1990) 1867.
[14] D.L. Smith, H. Evans, C. Smith, et al., in: Zs. Kajcsos, Cs. Szeles (Eds.), Proc. 9th Int. Conf. on Positron Annihilation, Szombathely, Hungary, August 26, 1991, Trans Tech Publications, Switzerland, 1992, Vol. 105–107, P. 1451.
[15] R.S. Brusa, M. Duarte Naia, A. Zecca, et al., Phys. Rev. B 49 (1994) 7271.